We are IntechOpen, the world's leading publisher of Open Access books
Built by scientists, for scientists

6,900
Open access books available

185,000
International authors and editors

200M
Downloads

154
Countries delivered to

Our authors are among the

TOP 1%
most cited scientists

12.2%
Contributors from top 500 universities

CLARIVATE ANALYTICS
BOOK CITATION INDEX
INDEXED

WEB OF SCIENCE™

Selection of our books indexed in the Book Citation Index
in Web of Science™ Core Collection (BKCI)

Interested in publishing with us?
Contact book.department@intechopen.com

Numbers displayed above are based on latest data collected.
For more information visit www.intechopen.com

Residual Stress Evaluation with Contour Method for Thick Butt Welded Joint

Qingya Zhang, Hong Zhou and Jiangchao Wang

Abstract

Thick plate with high tensile strength steel is increasingly employed for offshore structure fabrication, and welding residual stress is essential for assessment of mechanical performance and fatigue toughness. Therefore, it has been becoming the research issue to evaluate the distribution and magnitude of welding residual stress during butt welding of thick plate. With its advantages, contour method (CM) can be used for longitudinal residual stress evaluation by means of measuring sectional shrinkage after cutting the butt welded joint perpendicular to the welding line. Meanwhile, inverse finite element method (IFEM) code is programmed with C++ language to analyze the measured data to reestablish the welding residual stress. And based on the parallel computation of high-performance server, considering the effect of weld remelting and back-gouging during multi-pass welding process, the welding residual stress is predicted by using efficient thermal elastic plastic finite element method (TEP FEM). Results show that longitudinal residual stress turned from tensile stress in welded vicinity into compressive stress in base metal and the maximum tensile stress is 269 MPa. The computed longitudinal residual stress and welding displacement through TEP FEM are identified with the experimental results. In addition, the back-gouging has an insignificant effect on the residual stress but increases the welding displacement of butt welded joint. The proposed TEP FEM can accurately predict the welding residual stress in welded joint and is also an effective method to control welding displacement.

Keywords: high tensile strength steel, residual stress, CM, IFEM

1. Introduction

With the rapid development of lightweight fabrication in ship industry, thick plate with high tensile strength steel was increasingly employed for marine and offshore structure fabrication [1]. Welding technology with high efficiency is an indispensable process used for ship and offshore fabrication. However, it is inevitable that the residual stress of the welded joint and/or structure was induced by welding. Welding residual stresses can be defined as self-equilibrating stresses in a welded component with the absence of external load [2, 3]. It is known to us all that they can interact with imposed stresses and affect the service performance and structural integrity of welded components. Reliable knowledge of welding residual stress is essential to investigate the root cause of degradation mechanism, carry out

structural integrity assessment for safety critical components, optimize the design of manufacturing routes, and validate residual stress predictions [4, 5].

Up to now, several qualitative and quantitative techniques have been developed to measure residual stress, which are determined by using the specific elastic constants of material based on the measured strain rather than measured stress. All of them are divided into two categories: destructive techniques and nondestructive techniques [6]. For destructive techniques such as sectioning method, hole drilling method, and CM, the residual stress is measured by its relaxation due to the destruction of the state of the equilibrium of residual stress in a mechanical component. While for nondestructive techniques such as X-ray diffraction method and neutron diffraction method, residual stress is determined based on the relationship between residual stress crystallographic parameters of the material. Among the techniques above, according to the Bueckner's superposition principle, CM can provide a 2D cross-sectional map of residual stress normal to a plane of interest which combines the stress relaxation technology and finite element method [7]. The standard procedure of CM is implemented by the following steps [8]: (1) sample cutting on a plane of interest, (2) contour measurement of the cutting plane or surface, (3) data processing of the measurement results, and (4) residual stress back-calculation by using finite element analysis. CM has found a lot of literatures: Xie [9] estimated the residual stress in thick Ti-6Al-4V alloy welded joint by electron beam welding through finite element method and contour method. Murugan and Narayanan [10] employed both the finite element method and contour method to reveal the residual stress distribution induced by welding in tee joint and found that the experimental results agree well with the predicted stress. What's more, Turski and Edwards [11] efficiently measured the residual stress of 316L stainless steel by utilizing the contour method. Braga et al. [12] studied the welding residual stress profile of butt joints of S355 structural steel through contour method and neutron diffraction. Kainuma [13] investigated the welding residual stress in orthotropic steel decks which had a considerable effect on crack initiation and propagation by using cutting method and magnetostriction method. Woo [14] obtained the two-dimensional maps of the longitudinal residual stress through the thickness of 70-mm thick ferritic steel by using the CM. After that, Woo [15] determined the residual stress in an 80-mm thick ferritic steel by combining the neutron diffraction and CM. In addition to butt welded joint, Liu [16] measured the internal residual stress on inertia friction welding of nickel-based superalloy.

From the reviews above, the CM has obtained a lot of achievements. However, the accuracy of novel embedded cutting contour configuration for thick plate welded joint has not been evaluated. In this paper, the welding residual stress of 30-mm thick plate butt welded joint was investigated combining TEP FEM and CM. What's more, the effect of back-gouging on the residual stress distribution of butt welded joint was discussed.

2. Prediction of welding residual stress by TEP FEM

In this study, the welding residual stress in the butt welded joint through shielded metal arc welding (SMAW) was predicted by TEP FEM, an uncoupled thermal/mechanical formulation procedure, which is mainly composed of two sections: (a) the thermal analysis process and (b) the stress analysis process. Because the former has decisive effect on the latter while the latter has only a small influence on the former, thermal-mechanical behavior during welding is analyzed by using uncoupled thermal/mechanical formulation [17]. During thermal analysis, the 3D

welded joint FE model is established firstly using the solid element model according to the dimension of welded joint. The heat source model is considered to be an important aspect, and the double-ellipsoidal volumetric model is employed to simulate the welding transient temperature [18]. The heat flux is determined by the welding current, welding voltage, and welding speed. Besides considering the moving heat source, heat loss due to convection and radiation should also be taken into account in the thermal analysis. And the temperature-dependent thermal properties such as thermal conductivity, specific heat, and density are used.

The mechanical analysis is conducted using the welding temperature histories by thermal analysis as the input load. The same FE model used in thermal analysis is employed here. For mechanical analysis, temperature-dependent mechanical properties such as Poisson's ratio, yield strength, Young's modulus, and linear expansion coefficient are mainly considered. Moreover, the total strain was a summation of the elastic strain, thermal strain, plastic strain, creep strain, and strain induced by phase transformation during welding process, as was shown by Eq. (1). The thermal strain is considered using thermal expansion coefficient, and solid-state phase transformation has insignificant influence on the residual stress and deformation in the mild steel [19], so phase change was neglected in the present study. In addition, because the period with high temperature during the entire thermal cycle was very short (only a few seconds), the creep behavior was also ignored. In addition, the working hardening is neglected in this study since its effect on welding residual stress is not significant for mild steel. The total strain increment at a material point can be expressed as the summation of elastic, plastic, and thermal strains, as was shown by Eq. (2):

$$\varepsilon^{total} = \varepsilon^{elastic} + \varepsilon^{thermal} + \varepsilon^{phase} + \varepsilon^{plastic} + \varepsilon^{creep} \qquad (1)$$

$$\varepsilon^{total} = \varepsilon^{elastic} + \varepsilon^{thermal} + \varepsilon^{plastic} \qquad (2)$$

To ensure the weld fully penetrated, carbon arc gouging process is usually used to remove root metal. In principle, the root metal was melted by carbon arc and blown away by high pressured gas, increasing the original weld area and changing cross-section weld appearance. In this paper, it assumes that the welding arc plays the same role like carbon arc. Therefore, to investigate the effect of back-gouging on residual stresses in butt welded joint, the root weld bead of main weld was heated again when heating back weld.

3. Experimental procedure

In this section, the experimental procedure was introduced: the first step was to obtain the butt welded joint, and then the out-of-plane welding displacement was measured; the next step was to measure the welding residual stress through CM. Finally, the weld profile of cross-section was obtained.

3.1 Welding work

In this study, the butt welded joint was obtained by SMAW. In detail, the low carbon steel Q235 with the thickness of 30 mm was used as base metal, and the filler metal was J507 welding rod with the diameter of 4 mm. The welding groove was symmetric with the angle of 60°. The detailed dimensions and weld groove are presented in **Figure 1**.

3.2 CM measuring principle

On the basis of the Bueckner's superposition principle, the CM is applied for evaluating residual stress existing in metallic parts or structures. The ideal theoretical implementation of CM used for weld is displayed in **Figure 2**. Step A in **Figure 2** is the undisturbed welded joint and the residual stress that one wishes to determine. In step B, the part was cut in two on the plane x = 0 and the cutting plane deformed due to the near-surface residual stress fully released by the cut; therefore stress in the plane x = 0 was zero. Step C is an analytical step, in which the deformed cut surface is forced back to its original shape; the resulting change in stress is determined. Superimposing the stress state in B with the change in stress from C gives the original residual stress throughout the part. And for arbitrary plane in weld, its residual stress can be determined by the following general expression:

$$\sigma^A_{(x,y,z)} = \sigma^B_{(x,y,z)} + \sigma^C_{(x,y,z)} \tag{3}$$

3.3 CM measurement procedure

3.3.1 Welded specimen cutting

Welded specimen cutting is the first and most important step during the CM procedure as the subsequent steps of surface measurement, data processing, and stress calculation rely on the cutting quality of surface contour. It assumes that the
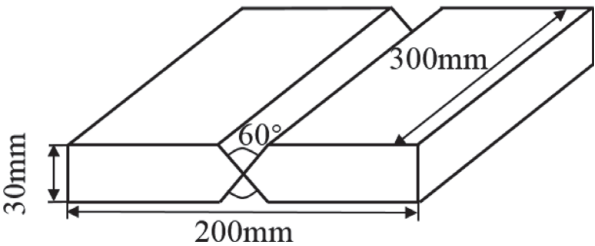

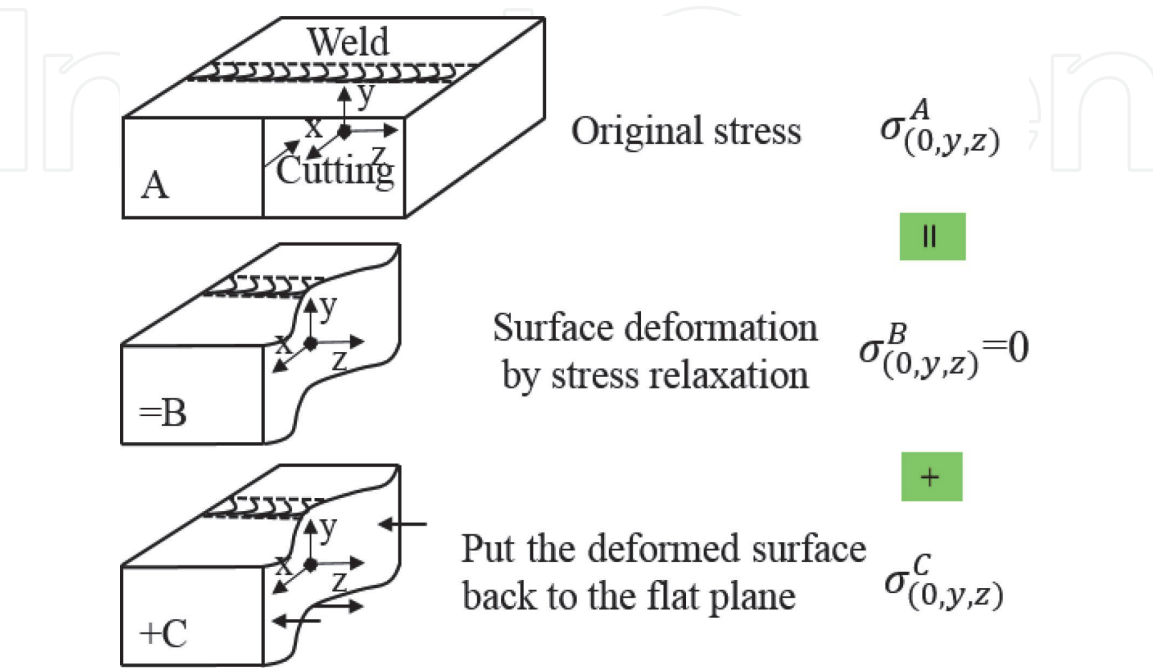**Figure 1.**
Weld groove and dimensions.

Figure 2.
Schematic diagram of the CM.

4

cutting process relaxes the residual stress elastically and does not induce any stress into the material. At present, cutting process is implemented by using the wire electrical discharge machining (WEDM) as it can generate a perfectly straight cut and does not remove any further material from the cut surfaces. "Skim cut" setting is used in order to minimize the effect of cutting process on the contour displacement during the relaxation of residual stress. The "skim" mode of WEDM cutting is preferred for contour cuts because of the lower roughness this setting produces. After setting the cutting parameters, the welded specimen is submerged in temperature-controlled deionized water during cutting. In this study, the Sodick AQ400LS with the wire diameter of 0.25 mm is used, and the cutting speed is 0.3 mm/min.

Additionally, in order to minimize the amount of cutting deviates from the original plane, welded specimens should be constrained from moving as stresses are released during the cutting. In conventional (**Figure 3a**) cut configuration, the effects of cutting errors and cutting artifacts cannot be neglected. In Hosseinzadeh's study, plasticity-induced errors in contour measurements can be mitigated by controlling the magnitude of the SIF during cutting. This can be done by choosing an appropriate cutting and restraint strategy. And the SIF is reduced by undertaking an "embedded cut" [20, 21]. Therefore, to mitigate the effects to some extent by restraining the "mode I" opening of cut surfaces during cutting, the embedded cut (**Figure 3b**) is used in this study.

3.3.2 Surface contour measurement

After the welded specimen cutting, the out-of-plane displacement can be implemented through contact measurement and non-contact measurement. Optical machines such as triangulating laser probes, confocal microscopes, et al. are useful for surface measurement. However, handling the large data sets, these systems produced can be problematic, usually requiring some sort of data reduction process. Comparing to non-contact measurement by optical machine, the coordinate measuring machine (CMM) with the uniform measured data is extensively employed for the contour measurement because the regular measured point can be obtained. In this study, the Hexagon micro plus is equipped with a 5-mm diameter touch probe, as is illustrated in **Figure 4**. And each cut surface was sampled with a measurement point spacing of 1×1 mm.

3.3.3 Data processing

The procedure of measured data processing is data alignment, data smoothing, averaging of the two data sets, and fitting of the two data sets. The data alignment is
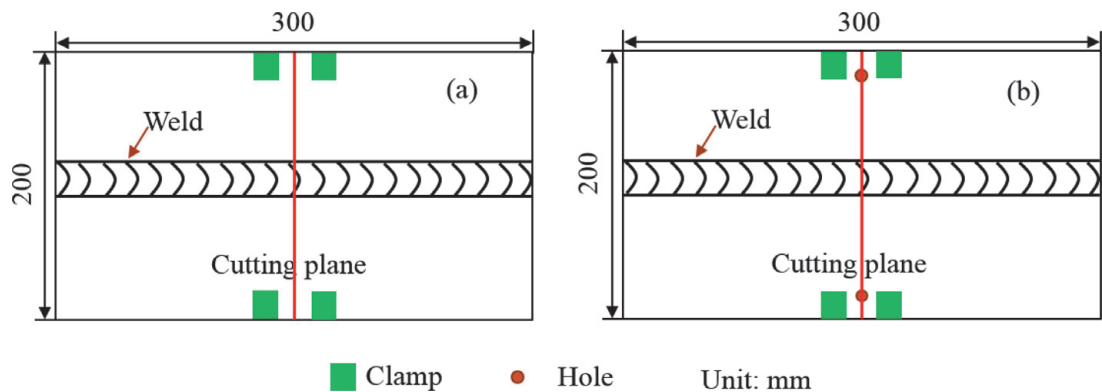

Figure 3.
Schematic drawing of contour cut configuration for welded specimens: (a) conventional contour cut configuration; (b) embedded cut.
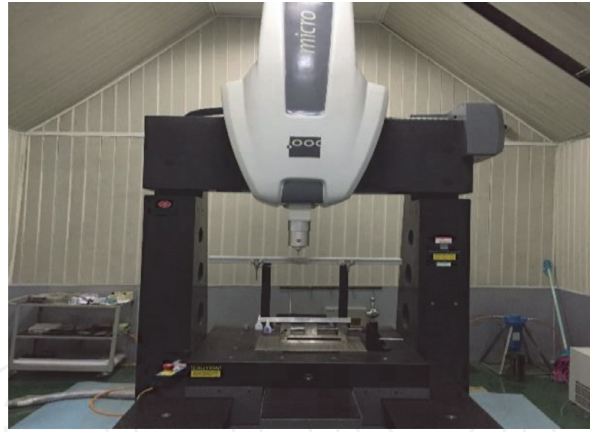
Figure 4.
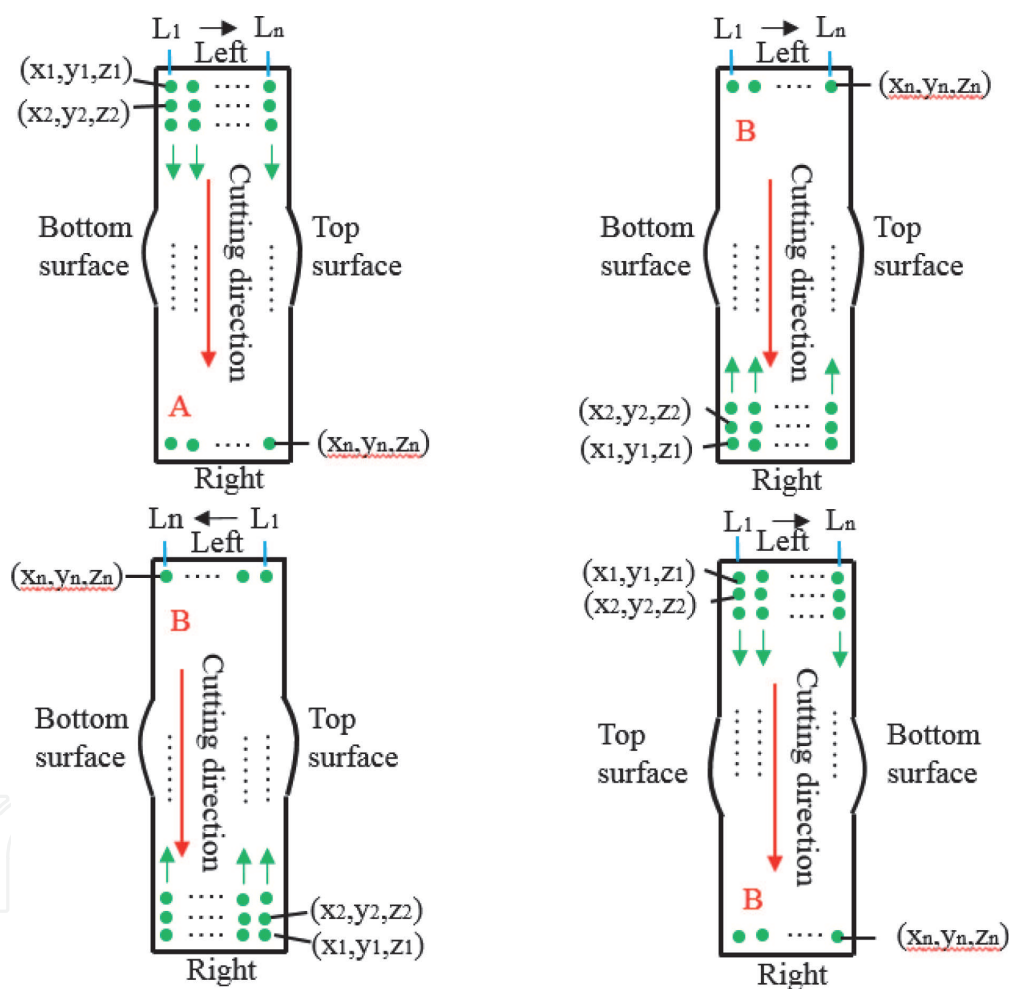*Hexagon coordinate measuring machine.*

Figure 5.
Data alignment according to the measurement data sequence.

to ensure the raw data on a regular rigid and at the same location. It can be seen from **Figure 5** that during surface contour measurement, several measuring sequence may occur. With the starting point and measuring direction marked, the data in surface B will be the same in surface A by data transposed in Excel or Matlab. Since the presence of noise and outliers is inevitable within the measured raw data, leading to the significant errors in the calculated stresses, the noise and outliers have to be smoothed prior to being applied as the nodal displacement condition in the linear elastic finite element analysis. The averaging of the two data sets can cancel out the shear stress effects and other errors. Fitting of the two data

sets can be conducted by spline, Fourier, or polynomial. In this study, the "sgolay" method was used to remove noise and outliers and also fit the measured data through Matlab: the processed data was displayed in **Figure 6**.

3.3.4 Stress calculation

In the final step of CM, the residual stress normal to a plane of interest can be obtained by linear elastic finite element analysis. In this step, the negative processed
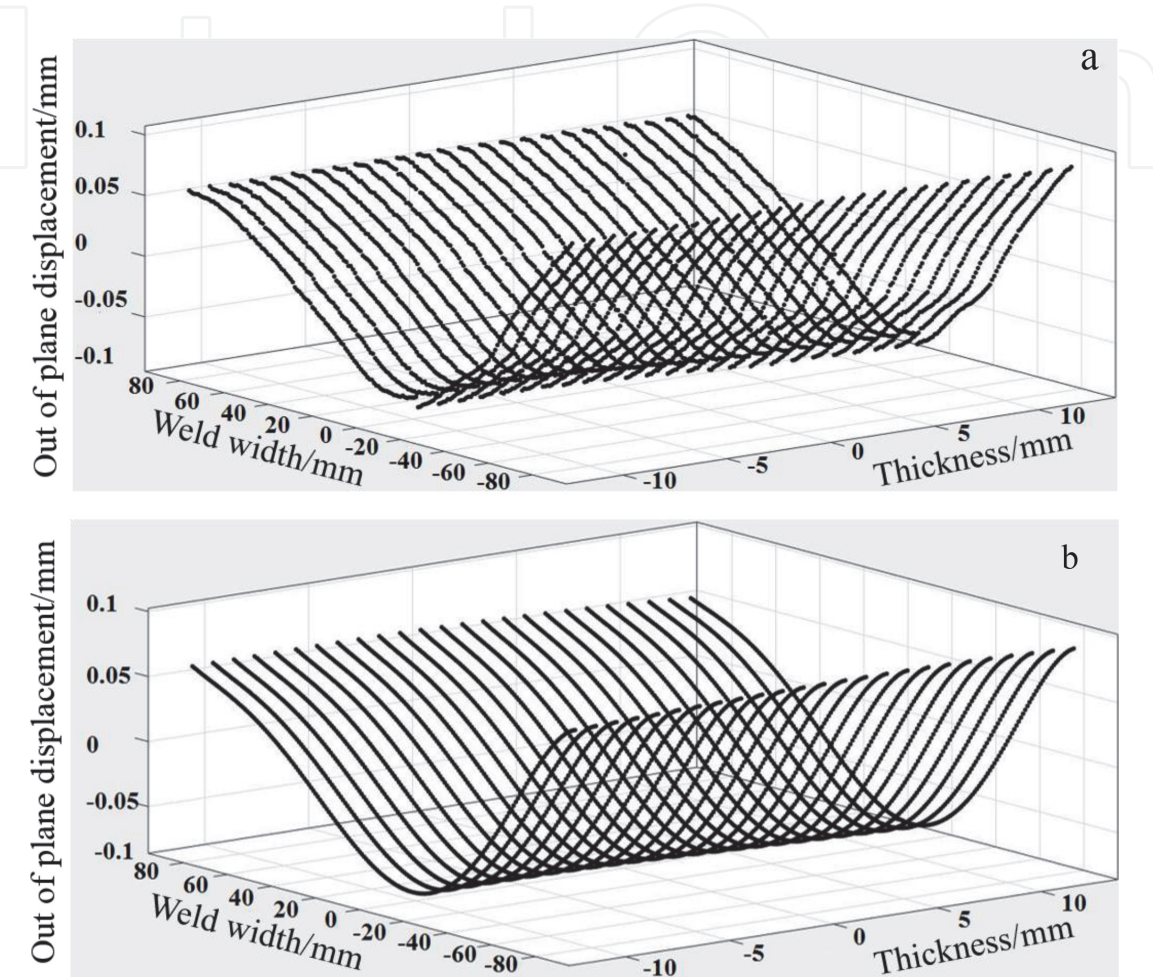

Figure 6.
The processed data of contour: (a) raw data after average; (b) after processing.
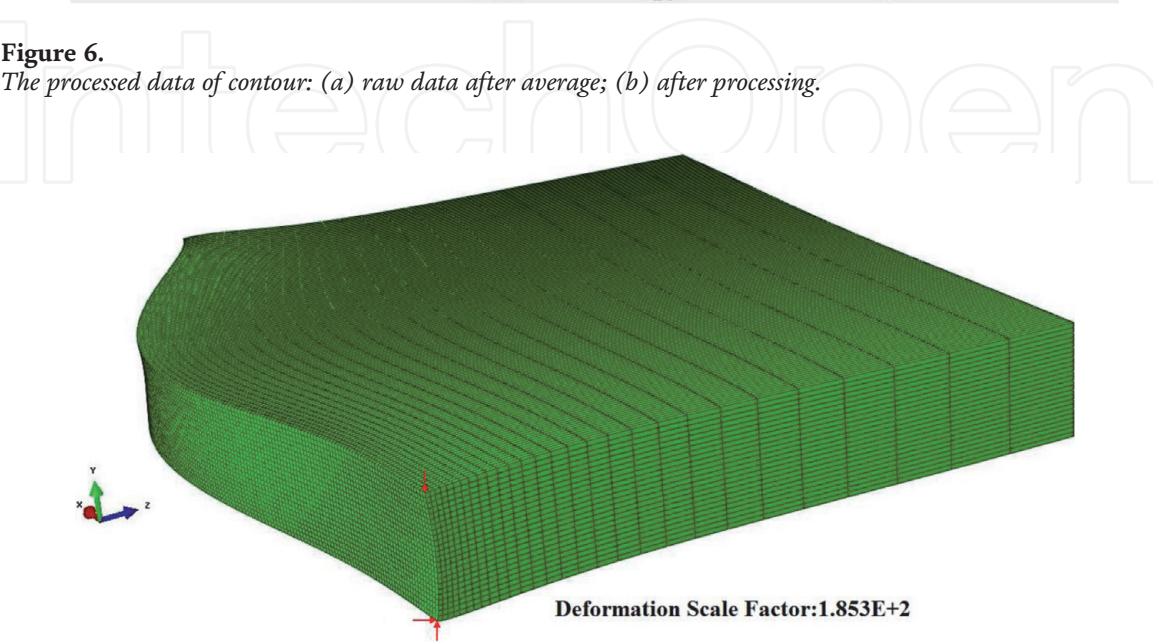
Figure 7.
Finite element model for linear elastic analysis.

data is applied as the nodal displacement condition of the finite element model which is often created according to the half of the whole welded specimen by using ABAQUS or ANSYS code. **Figure 7** displayed the finite element model of half welded joint, and red arrows representing boundary condition prevented the movement of rigid body. The inverse of the measured contour has been applied to the cut surface (deformation in this figure has been magnified ×185). A fine element size (1 mm) is that faces the cutting surface in addition to a fine mesh density around the cutting plane are used in the present FE model.

4. IFEM

According to the concept of CM, the residual stress existing in welded specimens can be calculated through the measured out-of-plane displacement normal to a plane of interest. Several assumptions are made in the linear elastic finite element analysis: (1) small displacements or deformations of the welded components or structures, (2) linear elastic behavior during the material removal, and (3) unchanged boundary conditions during loading process. Therefore, it can be defined as an inverse finite element method (IFEM). In general, a set of linear equation below describes the welded components or structures in the linear elastic finite element:

$$[K][u] = [F] \qquad (4)$$

$$[K] = \frac{E}{(1-2v)(1+v)} \begin{bmatrix} \frac{\partial^2(1-v)}{\partial x^2} + \left(\frac{\partial^2}{\partial y^2} + \frac{\partial^2}{\partial z^2}\right)\frac{(1-2v)}{2} & \frac{\partial^2}{2\partial x \partial y} & \frac{\partial^2}{2\partial x \partial z} \\ \frac{\partial^2}{2\partial x \partial y} & \frac{\partial^2(1-v)}{\partial y^2} + \left(\frac{\partial^2}{\partial x^2} + \frac{\partial^2}{\partial z^2}\right)\frac{(1-2v)}{2} & \frac{\partial^2}{2\partial y \partial z} \\ \frac{\partial^2}{2\partial x \partial z} & \frac{\partial^2}{2\partial y \partial z} & \frac{\partial^2(1-v)}{\partial z^2} + \left(\frac{\partial^2}{\partial x^2} + \frac{\partial^2}{\partial y^2}\right)\frac{(1-2v)}{2} \end{bmatrix}$$

where E is the Young's modulus, 210 GPa, v is Poisson's ratio, 0.3, $[K]$ is the stiffness matrix of the welded component or structure, $[u]$ is the matrix of nodal displacements, and $[F]$ is the matrix of external nodal force.

5. Results and discussion

The experimental results and simulation results were discussed in section. Based on the reliable welding temperature simulation, the longitudinal residual stress through TEP FEM and CM was analyzed. After that the transverse welding residual stress through TEP FEM was obtained. The comparison analysis of welding displacement was conducted to further validate the efficiency and accuracy of the proposed TEP FEM.

5.1 Maximum welding temperature distribution

Figure 8 displays two FEM models of the butt welded joint, which contain 13,702 nodes, 12,300 elements and 22,072 nodes, 20,400 elements, respectively, and the mechanical boundary constraint conditions are displayed in **Figure 8** by the arrows. It can be evidently seen from the picture that there are a large amount of nodes in the vicinity of weld and mesh toward the plate edge gradually reduced. The way of mesh arrangement is useful for improving computation efficiency and
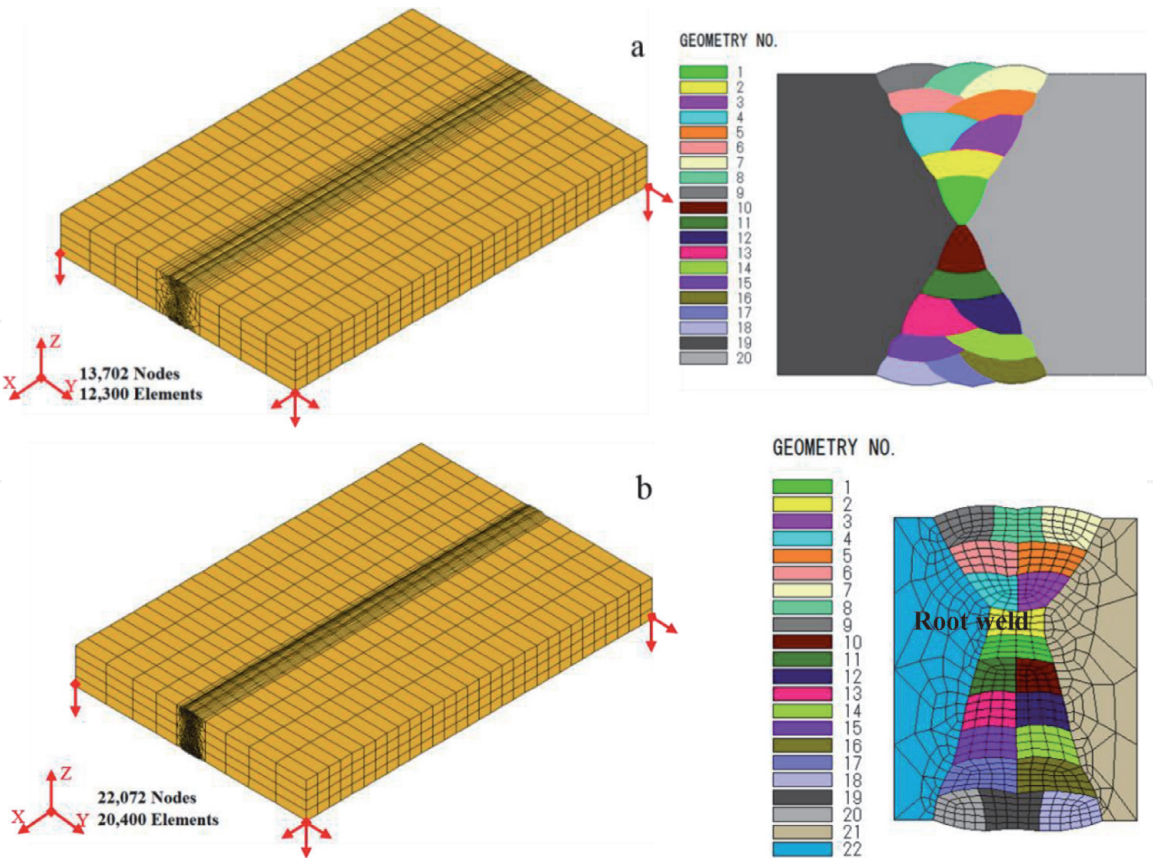
Figure 8.
Simulation model and weld sequence of butt welded joint: (a) without considering back-gouging; (b) with considering back-gouging.

ensuring computation accuracy when carrying out transient welding temperature nonlinear heat transfer computation.

5.1.1 Root weld

In principle, plastic strain is the generation source of welding residual stress, which is mainly determined by the maximum welding temperature and restraint condition. Here, the restraint condition is not considered, and the maximum welding temperature distribution is used to describe the features of welding temperature field of the butt welded joint. During the thermal analysis of the butt welded joint, the initial temperature is assumed to be 20°C. To simulate the heat input of moving welding arc during welding, the volumetric heat source with uniform density distribution is employed. For this heat source, the welding arc energy is dependent on the welding current, voltage, speed, and arc efficiency. When the welding process is SMAW, the arc heat efficiency is 0.6 and the welding arc length is 30 mm. And the heat source volume denoted the considered weld pool volume and can be obtained by calculating the volume fraction of the elements in currently being welded zone. The nonlinear isotropic Fourier heat flux was also employed for heat conduction. The temperature-dependent thermal properties such as thermal conductivity, specific heat, and density are considered. **Figure 9** presents the fusion zone in middle cross-section of the butt welded joint with or without considering back-gouging. The simulated fusion zone is slightly greater than the X-groove area, while the maximum temperature is approximately 2300°C. Comparing to the macrostructure of the butt welded joint, the fusion zone with considering back-gouging agrees better than that without considering back-gouging. Therefore,
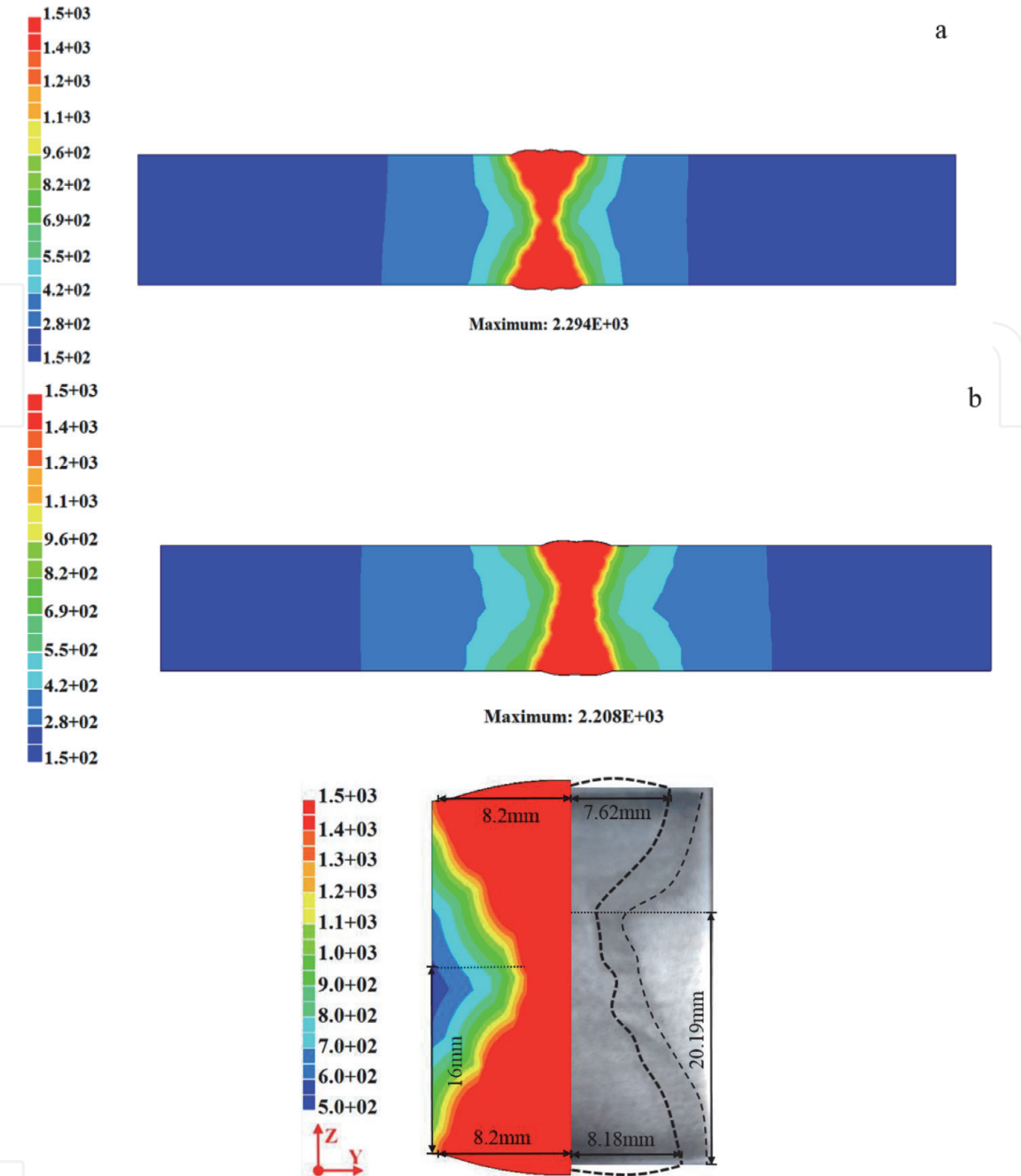
Figure 9.
Fusion zone of butt welded joint: (a) without considering back-gouging; (b) with considering back-gouging.

it can be concluded that the fusion area predicted by FEM with considering back-gouging is reasonable.

5.2 Welding residual stress distribution

Figure 10a–c displays the 2D mapping of longitudinal welding residual stresses in the middle cross-section computed by the numerical simulation and IFEM, respectively. In detail, **Figure 10a** presents the longitudinal residual stresses without considering back-gouging, **Figure 10b** shows the longitudinal residual stresses with considering back-gouging, and **Figure 10c** illustrates the longitudinal residual stresses by IFEM. It can be seen from the figure that both the longitudinal residual stresses with or without considering back-gouging matched with the measured contour. But, the peak value of longitudinal residual stress with considering back-gouging is higher than that without considering back-gouging, which is almost equal to the maximum measured value. Moreover, back-gouging process can reduce
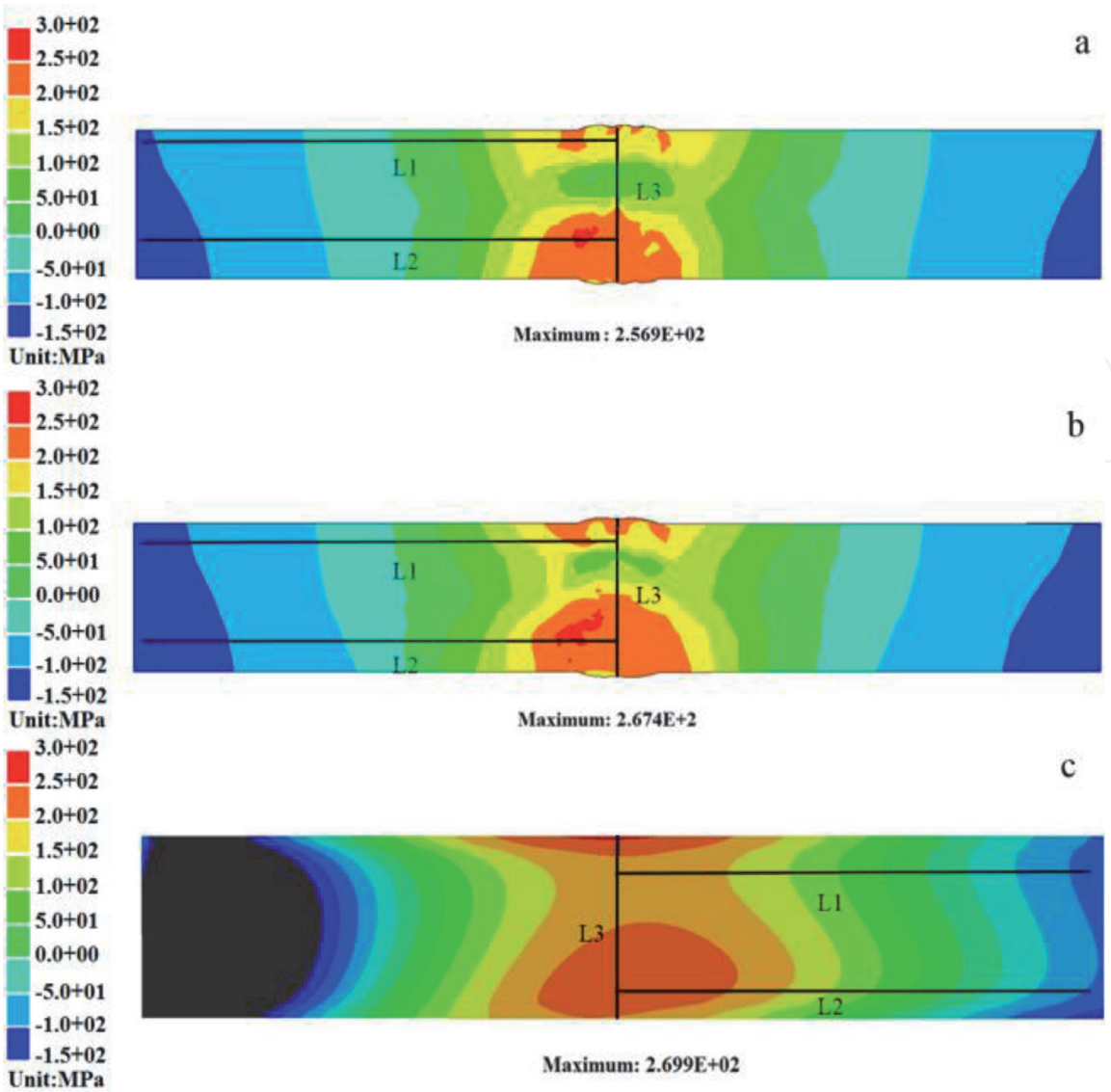
Figure 10.
2D mapping of longitudinal welding residual stress distribution of middle cross-section: (a) without considering back-gouging; (b) with considering back-gouging; (c) IFEM.

the tensile stress area of main weld. In addition, **Figure 10c** shows some irregularities at the edges of the cut surfaces; these irregularities may be produced due to wire entrance and exit during the specimen cutting.

Figure 11a–c quantitatively compares the longitudinal welding residual stress distributions in the middle cross-section along L1, L2, and L3 computed by TEP FE and the corresponding measurements, respectively. It can be seen from the **Figure 11a, b** that the computed longitudinal residual stress distributions along L1 and L2 agree well with the measured stress distribution. It can be seen from **Figure 11c** that the through-thickness longitudinal stresses distribution in center weld was obviously smaller than that in cap welds, which can be increased by back-gouging process. Therefore, it can be found that the peak longitudinal stresses were in cap welds and the longitudinal stresses in center weld can be increased by back-gouging process.

Figure 12a, b displays the features of transverse residual stresses in butt welded joint with or without considering back-gouging, respectively. It can be seen from the picture that the tensile stress is almost constant, while the compressive stress considering back-gouging is greater than that without considering back-gouging. And the middle cross-section mappings show that the signal of transverse residual stresses of local root weld and its distribution are changed obviously. Finally, the
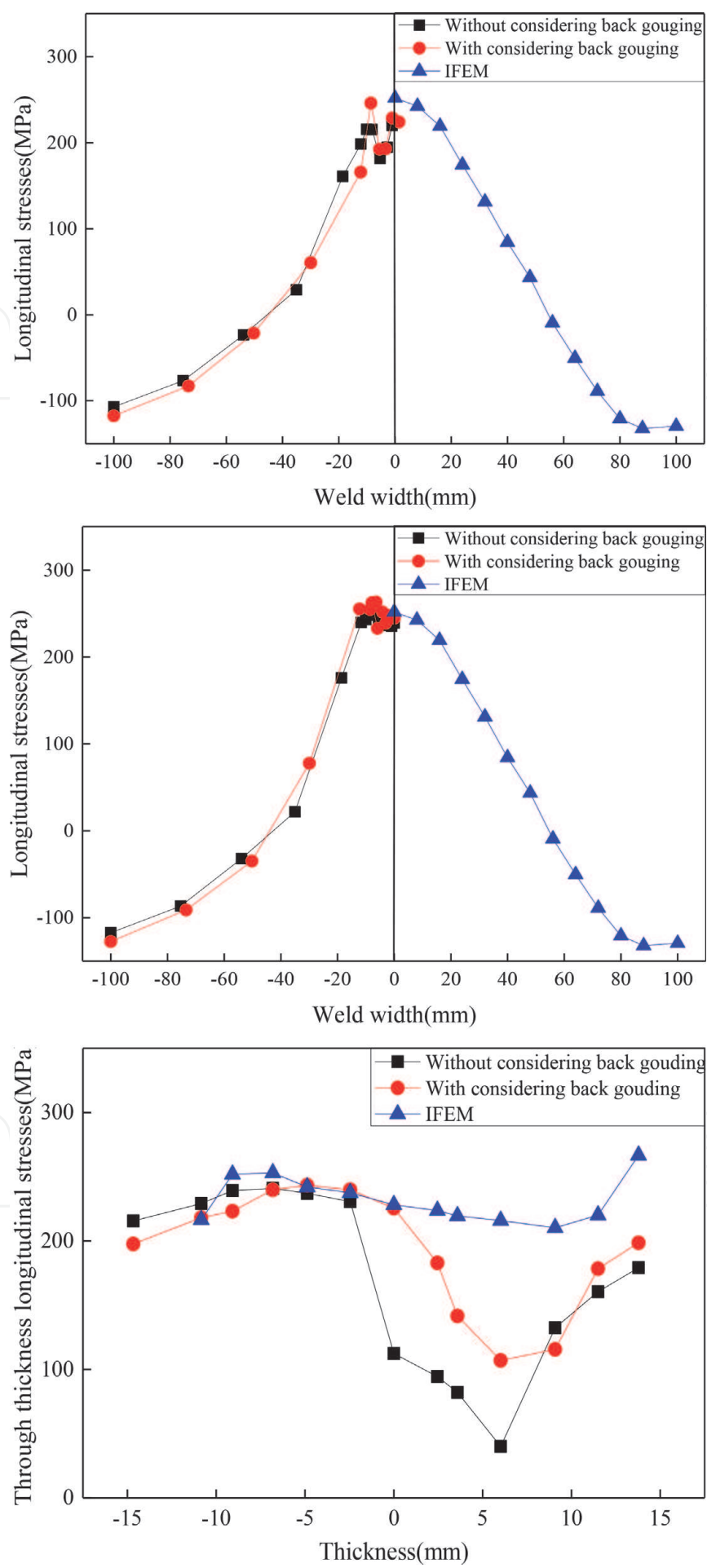
Figure 11.
Longitudinal residual stress distributions along L1, L2, and L3.

locations of the maximum residual stress and through-thickness spatial distributions provide an indication of the significance of crack initiation and the integrity of the welded components.

5.3 Welding displacement

Figure 13 showed the contour of z-direction welding displacement through TEP FEM and CMM measurement. The maximum z-direction welding displacement by TEP FEM was 0.9363 mm without considering back-gouging and 1.5874 with considering back-gouging, respectively. The maximum z-direction displacement by
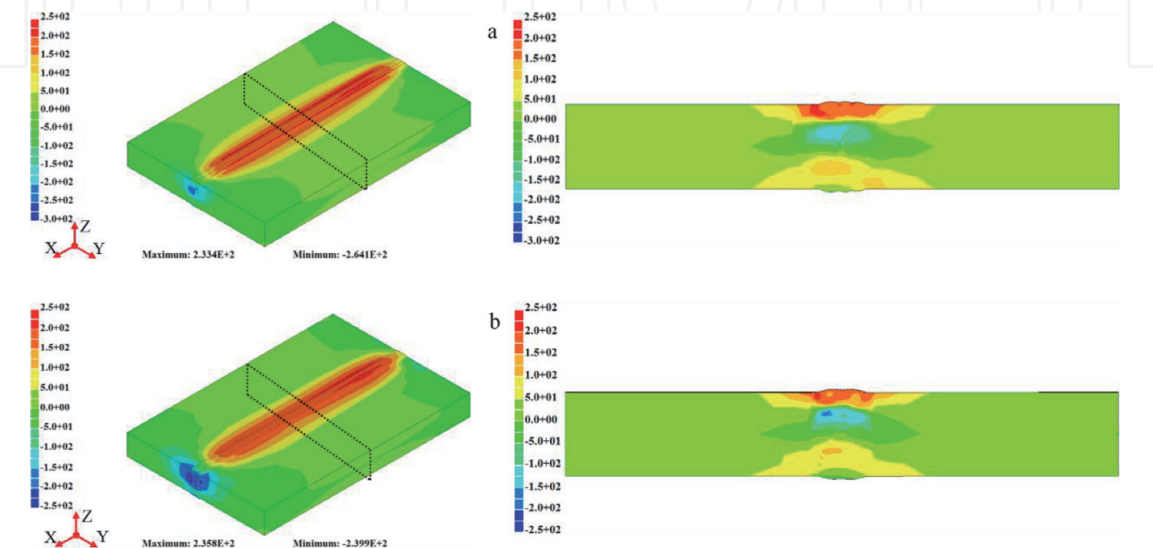
Figure 12.
Transverse welding residual stress distribution: (a) without considering back-gouging; (b) with considering back-gouging.
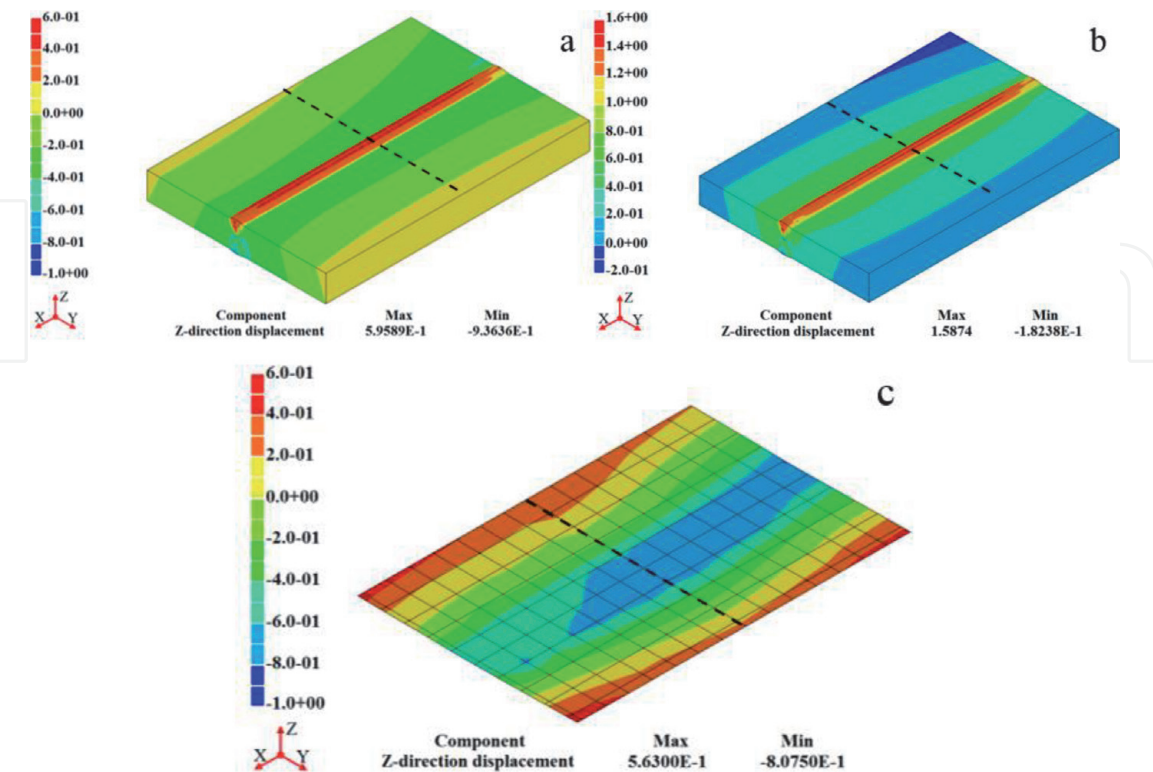

Figure 13.
Contour of z-direction welding displacement: (a) without considering back-gouging, (b) with considering back-gouging, and (c) experimental measurement.
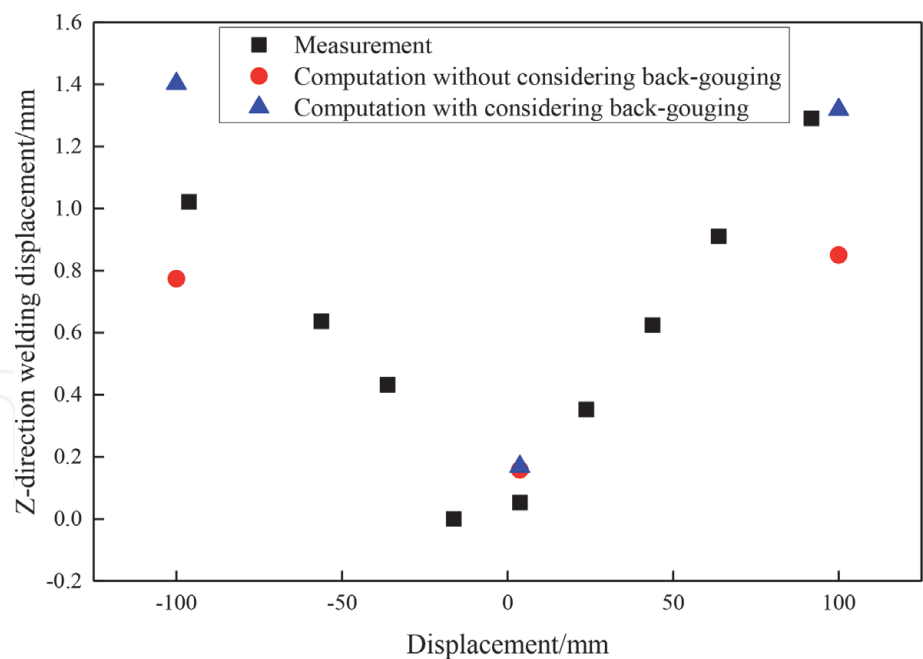
Figure 14.
Comparison of z-direction welding displacement.

CMM measurement was 0.80750. The quantitative analysis was carried out by extracting the mid-length displacement, as was displayed in **Figure 14**. Taking the weld center as the deformation base point, it can be seen that the computation of z-direction welding displacement considering back-gouging had a better agreement with the measurement. It is analyzed that the deformation after main welding was mitigated by the back-gouging process. Therefore, it can be concluded that the residual stress distribution and magnitude obtained by the efficient TEP FEM considering the back-gouging process were accurate and effective.

6. Conclusions

In this paper, the welding-induced residual stress in thick plate butt welded joint is evaluated through numerical simulation and CM. To validate the computed residual stresses, CM measurement is conducted. The results of the CM measurement are compared with the residual stresses computed by TEP FE. Based on the simulation and measured results, the following conclusions can be drawn:

1. Both the computed longitudinal residual stresses along weld width and through-thickness residual stresses are in a good agreement with the CM measured results.

2. Considering the back-gouging, the computed welding displacement through TEP FEM is identified with the measured result.

3. Through the comparison analysis of measurement and computation, the back-gouging has an insignificant effect on welding residual stress distribution and magnitude but can obviously increase the welding displacement.

Author details

Qingya Zhang[1,2], Hong Zhou[1] and Jiangchao Wang[2*]

1 School of Naval Architecture and Ocean Engineering, Jiangsu University of Science and Technology, Zhenjiang, China

2 School of Naval Architecture and Ocean Engineering, Huazhong University of Science and Technology, Wuhan, China

*Address all correspondence to: wangjiangchaocn@gmail.com

IntechOpen

References

[1] Wang JC, Zhao HQ, Zou JS, Zhou H, Wu ZF, Du SD. Welding distortion prediction with elastic FE analysis and mitigation practice in fabrication of cantilever beam component of jack-up drilling rig. Ocean Engineering. 2017; **130**:25-39

[2] Withers PJ, Bhadeshia HKDH. Residual stress. Part 1—Measurement techniques. Materials Science and Technology. 2001;**17**:355-365

[3] Withers PJ, Bhadeshia HKDH. Residual stress. Part 2—Nature and origins. Materials Science and Technology. 2001b;**17**:366-375

[4] Hosseinzadeh F, Kowal J, Bouchard PJ. Towards good practice guidelines for the contour method of residual stress measurement. The Journal of Engineering. 2014;**8**: 453-468

[5] Sun YL, Roy MJ, Vasileiou AN, Smith MC, Francis JA, Hosseinzadeh F. Evaluation of errors associated with cutting-induced plasticity in residual stress measurements using the contour method. Experimental Mechanics. 2017; **57**:719-734

[6] Withers PJ, Turski M, Edwards L, Bouchard PJ, Buttle DJ. Recent advances in residual stress measurement. International Journal of Pressure Vessels and Piping. 2008;**85**:118-127

[7] Prime MB. Cross-sectional mapping of residual stresses by measuring the surface contour after a cut. Journal of Engineering Materials and Technology. 2001;**123**:162-168

[8] Prime MB, DeWald AT. The contour method. In: Schajer GS, editor. Practical Residual Stress Measurement Methods. Hoboken, New Jersey, USA: John Wiley& Sons, Ltd; 2013. pp. 109-138

[9] Xie P, Zhao HY, Wu B, Gong SL. Using finite element and contour method to evaluate residual stress in thick Ti-6Al-4V alloy welded by electron beam welding. Acta Metallurgica Sinica (English Letters). 2015;**28**(7):922-930

[10] Murugan N, Narayanan R. Finite element simulation of residual stresses and their measurement by contour method. Materials & Design. 2009; **30**(6):2067-2071

[11] Turski M, Edwards L. Residual stress measurement of a 316l stainless steel bead-on-plate specimen utilising the contour method. International Journal of Pressure Vessels and Piping. 2009;**86**(1):126-151

[12] Braga DFO, Coules HE, Pirling T, Richter-Trummer V, Colegrove P, de Castro PMST. Assessment of residual stress of welded structural steel plates with or without post weld rolling using the contour method and neutron diffraction. Journal of Materials Processing Technology. 2013;**213**(12): 2323-2328

[13] Kainuma S, Jeong Y-S, Yang M, Inokuchi S. Welding residual stress in roots between deck plate and U-rib in orthotropic steel decks. Measurement. 2016;**92**:475-482

[14] Woo W, An GB, Kingston EJ, DeWald AT, Smith DJ, Hill MR. Through-thickness distributions of residual stresses in two extreme heat-input thick welds: A neutron diffraction, contour method and deep hole drilling study. Acta Materialia. 2013;**61**: 3564-3574

[15] Woo W, An GB, Em VT, De Wald AT, Hill MR. Through-thickness distributions of residual stresses in an 80 mm thick weld using

neutron diffraction and contour
method. Journal of Materials Science.
2015;**50**:784-793

[16] Liu C, Zhu H-Y, Dong C-L. Internal
residual stress measurement on inertia
friction welding of nickel-based super
alloy. Science and Technology of
Welding and Joining. 2014;**19**(5):
408-415

[17] Radaj D. Heat Effects of Welding:
Temperature Field, Residual Stress and
Distortion. Berlin/Heidelberg: Springer
Verlag Publishing; 1992

[18] Goldak JA, Akhlaghi M.
Computational Welding Mechanics.
Ottawa: Springer; 2005. pp. 71-115

[19] Yang YP, Dong P. Buckling
distortion and mitigation techniques for
thin section structures. Journal of
Materials Engineering and Performance.
2012;**21**(2):153-160

[20] Hosseinzadeh F, Traore Y,
Bouchard PJ, Muránsky O. Mitigating
cutting-induced plasticity in the contour
method. Part 1: Experimental.
International Journal of Solids and
Structures. 2016;**94–95**:247-253

[21] Muransky O, Hosseinzadeh F,
Hamelin CJ, Traore Y, Bendeich PJ.
Investigating optimal cutting
configurations for the contour method
of weld residual stress measurement.
International Journal of Pressure Vessels
and Piping. 2018;**164**:55-67